

Optimized Color Transforms for Image Demosaicing

Evgeny Gershikov

Department of Electrical Engineering, Ort Braude Academic College of Engineering,
Karmiel 21982, Israel
and Department of Electrical Engineering, Technion - IIT, Haifa 32000, Israel

Abstract:

Most demosaicing algorithms today are based on first reconstructing the green (G) color component followed by the reconstruction of the red (R) and the blue (B) components based on the green. This approach and the associated methods of using the differences $R-G$ and $B-G$ are arbitrary and in most cases not optimal. Instead, we propose optimal color transforms for demosaicing. This optimization is based on energy compactness and smoothness of the color components. We compare the performance of the proposed algorithms to presently available demosaicing methods and show that the new optimized approaches are superior both visually and quantitatively. Our conclusion is that the proposed color transforms improve the performance of demosaicing algorithms.

Keywords: Bayer pattern, Color transform, Demosaicing, Energy compactness, Image interpolation, Optimization, Smoothness

1. Introduction

Since many acquisition devices are based on a single sensor using a color filter array (CFA), only partially sampled versions of the primary colors R, G, B are recorded. This is done in most cases according to the Bayer pattern [1], as shown in Fig. 1. In this case, the green has twice as much samples as the red and the blue, making the green interpolation easier to accomplish due to reduced potential of aliasing [2,3]. Then the red and the blue components can be reconstructed based on inter-color correlations, which are usually high in natural images [4-8]. Straightforward algorithms for demosaicing, such as bilinear or bicubic interpolation methods, however, do not use these inter-color correlations and operate on each color component independently. Better performance is achieved by algorithms that are based on the above sequential scenario of reconstructing G first, followed by the reconstruction of R and B, e.g., [9-14]. In such algorithms the inter-color correlations are usually exploited by interpolating the differences $R-G$ and $B-G$. However, since no optimization is performed, it can be shown that using these differences is not the best method to perform the task efficiently. For the sake of completeness, we should add that non-sequential demosaicing methods have also been proposed, e.g. the iterative techniques of [15] or [16] as well as vector CFA demosaicing [17]. In this work we propose methods of choosing other color transforms for the interpolation of the red and the blue according to different optimization criteria.

We consider the following demosaicing algorithm.

1.1 The basic demosaicing algorithm

The stages of the algorithm are:

1. The green color component is interpolated using the method in [9]. It consists of filtering the CFA pattern horizontally and vertically, then choosing the direction of interpolation corresponding to the smaller estimated gradient (to avoid interpolation across edges): horizontal or vertical. In case of equal gradients the average of the horizontal and vertical interpolators is taken. This technique of interpolation was chosen because it provides good performance at low complexity.
2. The interpolated green component \hat{G} is used in the reconstruction of the red and the blue colors. The color differences $\Delta^{RG} \square R - \hat{G}$, $\Delta^{BG} \square B - \hat{G}$ are calculated at the known pixels of the red and the blue colors, respectively. Then the red-green difference is interpolated at the locations of the known blue samples and the blue-green difference at the locations of the red samples using the local polynomial approximation (LPA) filter [13]. Better performance can be achieved by this filter compared to simple bilinear interpolation.

- The missing pixels in the red and blue - those at the locations of the known green pixels are interpolated using simple averaging of their two vertical and two horizontal pixels (bilinear interpolation). The interpolation is performed once again on the Δ^{RG} and Δ^{BG} differences resulting in full images $\hat{\Delta}^{RG}$ and $\hat{\Delta}^{BG}$.

The final red and blue components are calculated according to $\hat{R} = \hat{G} + \hat{\Delta}^{RG}$ and

$$\hat{B} = \hat{G} + \hat{\Delta}^{BG}.$$

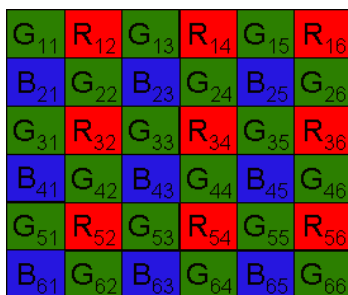


Figure 1. The Bayer CFA pattern.

The structure of this work is as follows. Color transforms for demosaicing based on optimization of different properties of the image are presented in Section 2. Demosaicing results for the proposed method and comparison to other available techniques are given in Section 3. Section 4 provides summary and conclusions.

2. Optimal Color Transforms

All printed material, including text, illustrations, and charts, must be kept within a print area of 6-1/2 inches (16.51 cm) wide by 8-7/8 inches (22.51 cm) high. Do not write or print anything outside the print area. All *text* must be in a single-column format. Columns are to be 3-1/16 inches (7.85 cm) wide, with The basic algorithm performs its interpolation in the $G, R - G, B - G$ color space. This choice is not necessarily optimal and thus other color transforms can be considered following an optimization process [18]. The change of the color space is not possible prior to the reconstruction of the green since at each pixel of the image only one of the primary colors is available. However, it becomes possible after the reconstruction of G in Subsection 1.1, Step 1. We thus propose a new general color space:

$$(1) C_1 = G, \quad C_2 = a_1R + a_2G, \quad C_3 = d_1B + d_2G$$

for some constants a_1, a_2, d_1, d_2 instead of the regular choice. To avoid the solution of $a_1 = a_2 = 0$ in the optimization problems presented below, a constraint has to be added forcing the L1 norm, for example, of the a coefficients to be 1 (similarly for the d coefficients). Thus

$$(2) |a_1| + |a_2| = 1 \quad \text{and} \quad |d_1| + |d_2| = 1.$$

2.1 Energy compactness and non-singularity

A Rate-Distortion model for color image coders was developed and optimized in [19]. As a result the optimal Color Transform (CT) was derived. Denoting the CT matrix by \mathbf{M} , the target function to be minimized for the optimal CT was found to be $\prod_{k=1}^3 \left((\mathbf{M}\mathbf{M}^T)^{-1} \right)_{kk} GM_k$, where GM_k is the geometric mean of the subband variances. Based on this result, the following target function can be proposed for our demosaicing algorithm:

$$(3) \prod_{k=2}^3 \left((\mathbf{M}\mathbf{M}^T)^{-1} \right)_{kk} var(C_k),$$

where C_k and the RGB components are connected by

$$(4) \quad \begin{bmatrix} C_1 \\ C_2 \\ C_3 \end{bmatrix} = \mathbf{M} \begin{bmatrix} R \\ G \\ B \end{bmatrix}, \quad \mathbf{M} = \begin{pmatrix} 0 & 1 & 0 \\ a_1 & a_2 & 0 \\ 0 & d_2 & d_1 \end{pmatrix}.$$

The expression in (3) is made of two terms: $\prod_{k=2}^3 \text{var}(C_k)$, which is a measure of the energy compactness in the new color space and $\prod_{k=2}^3 \left((\mathbf{M}\mathbf{M}^T)^{-1} \right)_{kk}$, which is a measure of the non-singularity of M. The optimal coefficients minimizing (3) under the norm constraint of (2) are

$$(5) \quad a_1 = \frac{\text{var}(G)}{\text{var}(G) + \text{cov}(R, G)}, \quad a_2 = -\frac{\text{cov}(R, G)}{\text{var}(G) + \text{cov}(R, G)}, \quad d_1 = \frac{\text{var}(G)}{\text{var}(G) + \text{cov}(B, G)}, \quad d_2 = -\frac{\text{cov}(B, G)}{\text{var}(G) + \text{cov}(B, G)}.$$

Since the target function of (3) combines the properties of energy compactness and non-singularity of the color transform, we refer to this algorithm as ECNS, which is the acronym of Energy Compactness and Non-Singularity.

2.2 Smoothness of the C2 and C3 components

The energy of the difference signals $\Delta^{RG} = R - G$ and $\Delta^{BG} = B - G$ is mostly concentrated in the low frequencies [11]. This is the reason for the good performance achieved by interpolating these differences using averaging [11-13]. This also means that Δ^{RG} and Δ^{BG} are smooth. To further impose this smoothness on C_2 and C_3 , the following methods are proposed.

2.2.1 Minimal high pass energy

The idea here is to minimize the energy of C_2 and C_3 , filtered by a two dimensional High Pass (HP) filter. We denote the filtered color components at pixel (i, j) by $(C_k^{HP})_{ij}$ and minimize $\sum_{i=1}^M \sum_{j=1}^N (C_k^{HP})_{ij}^2$, $k = 2, 3$ for an image of size $M \times N$. Alternatively, a pair of one dimensional HP filters HP_x and HP_y can be used to filter C_2 or C_3 horizontally and vertically, respectively. Usually, HP_y is chosen as $HP_y = HP_x^T$. Then the expression to be minimized becomes $\sum_i \sum_j (C_k^{HP_x})_{ij}^2 + \sum_i \sum_j (C_k^{HP_y})_{ij}^2$, $k = 2, 3$, where $C_k^{HP_x}$ is C_k filtered by HP_x and similarly for $C_k^{HP_y}$. The optimal a_1, a_2 coefficients for this problem are

$$(6) \quad a_1 = \frac{\alpha_{12} + \alpha_{22}}{\alpha_{11} + 2\alpha_{12} + \alpha_{22}}, \quad a_2 = -\frac{\alpha_{12} + \alpha_{11}}{\alpha_{11} + 2\alpha_{12} + \alpha_{22}},$$

where

$$(7) \quad \alpha_{11} \square \sum_i \sum_j \left[(R^{HP_x})_{ij}^2 + (R^{HP_y})_{ij}^2 \right], \quad \alpha_{22} \square \sum_i \sum_j \left[(G^{HP_x})_{ij}^2 + (G^{HP_y})_{ij}^2 \right], \\ \alpha_{12} \square \sum_i \sum_j \left[(R^{HP_x})_{ij} (G^{HP_x})_{ij} + (R^{HP_y})_{ij} (G^{HP_y})_{ij} \right].$$

The solution for the d_1 and d_2 coefficients is the same as the solution for a_1 and a_2 , respectively, in (6) with B replacing R everywhere in (7). For simple choices of HP_x , such as the backward/forward approximation of the horizontal derivative

($HP_x = [1 - 1]$), the calculations can be performed on the available small images obtained from the CFA (Fig. 2). Alternatively, R and B can be first reconstructed using a simple technique, such as bilinear filtering of the $R - G$ and $B - G$ differences, and then used for the estimation of the derivatives. In this work we use the Sobel

gradient operator given by $HP_x = \begin{pmatrix} 1 & 0 & -1 \\ 2 & 0 & -2 \\ 1 & 0 & -1 \end{pmatrix}$.

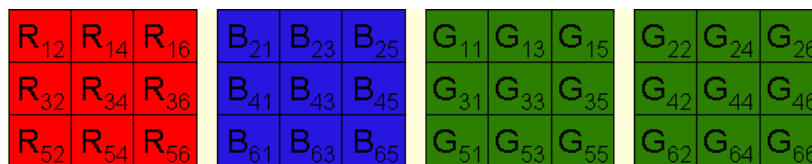


Figure 2. The Bayer pattern components: RR, BB, GR and GB (from left to right).

2.2.2 Minimal energy in the wavelet domain

Another approach is to consider the energy of the C_2 and C_3 color components in the high frequencies and to search for the coefficients a_k and d_k ($k = 2, 3$) that minimize this energy. One possible formulation for this problem is to minimize $\sum_{f \in \{LH, HL, HH\}} \sum_m \sum_n W_f^{C_k}(m, n)^2$, $k = 2, 3$, where $W_f^{C_k}(m, n)$ is the one level Discrete Wavelet Transform (DWT) of C_k at position (m, n) in subband f , which is one of the high frequency subbands (LH, HL or HH) above. The solution for this problem is as in (6), but now

$$(8) \quad \alpha_{11} \square \sum_{f \in \{LH, HL, HH\}} \sum_m \sum_n W_f^R(m, n)^2, \quad \alpha_{22} \square \sum_{f \in \{LH, HL, HH\}} \sum_m \sum_n W_f^G(m, n)^2,$$

$$\alpha_{12} \square \sum_{f \in \{LH, HL, HH\}} \sum_m \sum_n W_f^R(m, n) W_f^G(m, n).$$

The solution for d_1 and d_2 is similar.

2.2.3 Minimal relative energy in the Fourier domain

The energy in the high frequencies can be expressed in the frequency domain of the Discrete Fourier Transform (DFT) as well. In this case taking the relative energy of C_2 or C_3 provides better results. Therefore, we seek to minimize (for an image of size $M \times N$ assuming M and N are multiples of 4)

$$(9) \quad E \square \frac{\sum_{m=M/4}^{M/2-1} \sum_{n=N/4}^{N/2-1} |DFT^{C_k}(m, n)|^2}{\sum_{m=0}^{M/2-1} \sum_{n=0}^{N/2-1} |DFT^{C_k}(m, n)|^2}, \quad k = 2, 3.$$

$DFT^{C_k}(m, n)$ here denotes the DFT coefficient of C_k at position (m, n) in the frequency domain. The solution of this problem requires solving third order polynomial equations resulting in long expressions for the a and d coefficients. For simplicity we do not provide them here.

3. Demosaicing Results

The basic algorithm (Section 1.1) was implemented with and without the optimization techniques of Section 2. We also added the refinement method [20] as post-processing. This method provides further utilization of the inter-color and intra-color correlations and works well with our algorithms. The set of images given in Fig. 3 was used in our simulations, i.e., for each one the Bayer pattern was built, interpolated by the different algorithms and compared to the original image. The distortion measure used was the S-CIELAB metric [21]. The comparison of the proposed algorithms is given on the left side of Table 1. We can see that all the proposed algorithms achieve better results than the basic algorithm and the bilinear interpolation. The best performance with respect to the S-CIELAB metric is achieved by the minimal high pass energy (Min HP)

algorithm (Section 2.2.1). This shows the importance of the smoothness of the C_2 or C_3 color components for our interpolation process. The second best algorithm is ECNS, which means energy compactness and non-singularity of the color transform are important for demosaicing as well as image coding [18]. It is of interest to compare the proposed methods to other available algorithms. We have chosen some of the available state of the art techniques: Alternating Projections (AP [10]), Directional Linear Minimum Mean Square Error (DLMMSE [11]), Variance of Color Differences (VCD [12]), Local Polynomial Approximation (LPA [13]) and Successive Approximation (SAP [16]). The results for these algorithms can be seen on the right side of Table 1. From the table we can see that the Min HP algorithm is superior to the

other methods, while the performance of ECNS is similar to that of the VCD method that provides the best results among the algorithms chosen for comparison. Visual results for the new methods as well as existing algorithms for part of Image 8 are given in Fig. 4. As can be seen, the proposed methods provide better results than the other algorithms (including VCD that provides the most competitive performance). The values of the a and d coefficients for these algorithms are given in Table 2. Note that even if the values are close to $a_1 = -a_2 = 0.5$ and $d_1 = -d_2 = 0.5$, which would result in taking the common $R-G$ and $B-G$ differences (after scaling), the new methods outperform the basic algorithm.

4. Summary And Conclusions

An optimization approach to demosaicing has been introduced. Instead of using the common choice of the $R-G$ and $B-G$ differences for the reconstruction process, better performance can be achieved by choosing an optimized color space according to the desired properties of the image. Such properties can be energy compactness as in the ECNS algorithm or smoothness as in the Min HP algorithm. A basic demosaicing algorithm has been optimized to achieve these properties and compared to other available demosaicing methods. Our results show that the proposed optimization method significantly improves the interpolation performance and that the best performance is achieved by minimizing the high pass energy in the new color space. The second best is the algorithm that combines energy compactness and non-singularity of the color transform, providing better results also in the case of color image coding [18]. Our conclusion is that the proposed optimization approach is useful for demosaicing of color images.

Table 1. S-CIELAB results for the algorithms (from left to right): minimal High Pass energy, ECNS, minimal DWT energy, minimal relative DFT energy, the basic algorithm, bi-linear interpolation, AP, SAP, DLMMSE, LPA and VCD.

Image	Proposed Algorithms				Other Algorithms						
	Min HP	ECNS	Min DWT	Min Rel DFT	Basic	BL	AP	SAP	DL MMSE	LPA	VCD
1	0.733	0.729	0.752	0.730	0.769	1.505	0.851	0.897	0.723	0.758	0.850
2	0.779	0.786	0.794	0.830	0.796	1.201	1.032	1.215	0.749	0.766	0.778
3	0.747	0.732	0.791	0.812	0.808	1.501	1.165	1.177	0.832	0.832	0.795
4	0.645	0.654	0.650	0.659	0.656	0.833	0.787	0.877	0.644	0.611	0.687
5	0.579	0.595	0.571	0.593	0.578	0.928	0.838	0.828	0.561	0.530	0.593
6	0.576	0.611	0.594	0.577	0.606	1.149	0.654	0.760	0.524	0.581	0.526
7	1.408	1.475	1.456	1.467	1.488	3.272	1.862	1.810	1.431	1.321	1.312
8	1.490	1.508	1.569	1.569	1.608	2.742	1.867	2.168	1.689	2.154	1.563
Mean	0.870	0.886	0.897	0.905	0.914	1.641	1.132	1.216	0.894	0.944	0.888

Table 2. a and d coefficients for Image 8 for the proposed algorithms (same order of columns as in Table 1). Even if the values are close to $a_1 = -a_2 = 0.5$ and $d_1 = -d_2 = 0.5$ as in the basic method, the new methods outperform the basic algorithm.

	Min HP	ECNS	Min DWT	Min Rel DFT
a_1	0.539	0.578	0.506	0.460
a_2	-0.461	-0.422	-0.494	-0.540
d_1	0.551	0.597	0.509	0.559
d_2	-0.449	-0.403	-0.491	-0.441



Figure 3. The demosaicing test images.





Figure 4. Demosaicing results for the different algorithms for part of Image 8. New Alg. 1-4 are the new algorithms.

References

- [1] B. E. Bayer. Color imaging array. U.S. Patent 3971065, July 1976.
- [2] B. Gunturk, X. Li and L. Zhang. Image demosaicing: A systematic survey. In Proc. of SPIE, 68221J-68221J-15, 2008.
- [3] H. Kirshner and M. Porat. On the Approximation of L2 Inner Products from Sampled Data. IEEE Trans. on Signal Processing 55:2136-2144, 2007.
- [4] H. Kotera and K. Kanamori. A Novel Coding Algorithm for Representing Full Color Images by a Single Color Image. J. Imaging Technology 16:142-152, Aug. 1990.
- [5] J. O. Limb and C.B. Rubinstein. Statistical Dependence Between Components of A Differentially Quantized Color Signal. IEEE Trans. on Communications 20:890-899, Oct. 1971.
- [6] H. Yamaguchi. Efficient Encoding of Colored Pictures in R, G, B Components. IEEE Trans. on Communications 32:1201-1209, Nov. 1984.
- [7] Y. Roterman and M. Porat. Color image coding using regional correlation of primary colors. Image and Vision Computing 25:637-651, 2007.
- [8] E. Gershikov and M. Porat. Optimal color image compression using localized color component transforms. In Proc. EUSIPCO 2008, Lausanne, Switzerland, Aug. 2008.
- [9] J. F. Hamilton and J. E. Adams. Adaptive Color Plane Interpolation in Single Sensor Color Electronic Camera. U.S. Patent 5629734, 1997.
- [10] B. K. Gunturk, Y. Altunbasak, and R. M. Mersereau. Color plane interpolation using alternating projections. IEEE Trans. Image Processing 11:997-1013, 2002.
- [11] L. Zhang and X. Wu. Color demosaicking via directional linear minimum mean square-error estimation. IEEE Trans. on Image Processing 14:2167-2178, 2005.
- [12] K.-H. Chung and Y.-H. Chan. Color demosaicing using variance of color differences. IEEE Trans. on Image Processing 15:2944-2955, 2006.
- [13] D. Paliy, V. Katkovnik, R. Bilcu, S. Alenius, and K. Egiazarian. Spatially adaptive color filter array interpolation for noiseless and noisy data. Int. Journal of Imag. Sys. and Technology 17:105-122, 2007.
- [14] R. Sher and M. Porat. CCD Image Demosaicing using Localized Correlations. In Proc. of EUSIPCO, Poznan, Poland, Sept. 2007.
- [15] R. Kimmel. Demosaicing: Image reconstruction from color ccd samples. IEEE Trans. on Image Processing 8:1221-1228, 1999.
- [16] X. Li. Demosaicing by successive approximation. IEEE Trans. Image Processing 14:370-379.
- [17] M. R. Gupta and T. Chen. Vector color filter array demosaicing. In Proc. of SPIE, Sensors and Camera Systems for Scientific, Industrial, and Digital Photography Applications II 4306:374-382, 2001.
- [18] E. Gershikov and M. Porat. A rate-distortion approach to optimal color image compression. In Proc. EUSIPCO, Florence, Italy, Sept. 2006.
- [19] E. Gershikov and M. Porat. On color transforms and bit allocation for optimal subband image compression. Signal Processing: Image Communication 22:1-18, 2007.
- [20] L. Chang and Y. P. Tam. Effective use of spatial and spectral correlations for color filter array demosaicing. IEEE Trans. Consumer Electronics, 50:355-365, Feb 2004.
- [21] X. Zhang and B. A. Wandell. A spatial extension of CIELAB for digital color image reproduction. SID Journal 5:61-63, 1997.